

## Studying on mineralogical and petrological characteristics of Gara Djebilet oolitic iron ore, Tindouf (Algeria)

Nassima Chebel <sup>1</sup>, Djamel Nettour <sup>1</sup>, Mohamed Chettibi <sup>2</sup>, Rachid Chaib <sup>3</sup>, Hamid Khoshdast <sup>4,5</sup>, Ahmad Hassanzadeh <sup>6,7</sup>

<sup>1</sup> National Higher School of Technology and Engineering, Mines Metallurgy Materials Laboratory (L3M), 23005, Annaba, Algeria

<sup>2</sup> Laboratory Mineral Resources Valorization and Environment, Badji Mokhtar University, Annaba, Algeria

<sup>3</sup> Transportation Engineering Department, Laboratory of Transports and Environment Engineering, Mentouri Brothers University Constantine, Algeria

<sup>4</sup> Department of Mining Engineering, Higher Education Complex of Zarand, Shahid Bahonar University of Kerman, Kerman 7761156391, Iran

<sup>5</sup> Mineral Industries Research Center, Shahid Bahonar University of Kerman, 76169133 Kerman, Iran

<sup>6</sup> Department of Geoscience and Petroleum, Faculty of Engineering, Norwegian University of Science and Technology, Trondheim 7031, Norway

<sup>7</sup> Mineral Services Ltd, Ty Maelgwyn, 1 A Gower Road, Cathays, Cardiff CF244PA, United Kingdom

\*Corresponding authors: [n.chebel@etu.ensti-annaba.dz](mailto:n.chebel@etu.ensti-annaba.dz) (Nassima Chebel)

**Abstract:** Demand for iron ore worldwide has been steadily increasing which leads to the extraction of iron ore deposits with more complex mineralogies and higher levels of silicon and phosphorus impurities. This is the case in Algeria with the iron ore deposit of Gara Djebilet, Tindouf; where it has recently been exploited to ensure the sufficiency of iron ore required to produce iron and steel products. This deposit has remained unexploited for several decades due to inadequate knowledge of its mineralogy, treatment, and economic assessments. This study aims to find out the microstructure, chemical composition, and mineralogical distribution of valuable minerals and impurities, to understand the efficient processing methods for this specific iron ore. The characterization of representative ironstone samples taken from the studied area was carried out using optical microscopy, X-ray fluorescence spectrometer (XRF), petrographic microscope, X-ray diffractometer (XRD), and scanning electron microscope (SEM) coupled with energy dispersive X-ray spectroscopy (EDS). The results of the mineralogical analyses confirmed that it is an oolitic fine-grained ore consisting of gangue minerals principally composed of quartz, apatite, and iron-rich concentric cored structures. Chemical analyses of the ore indicated that it contains 56.58 wt% Fe with 7.98 wt% SiO<sub>2</sub>, 7.09 wt% Al<sub>2</sub>O<sub>3</sub>, and minor amounts of P<sub>2</sub>O<sub>5</sub>, CaO, MgO, and TiO<sub>2</sub> compounds. The phosphorus associated was present in both ooids and groundmass, indicating that the ore has a complex texture with very rich and diverse mineralogy. For that, two conceptual scenarios were potentially proposed for processing the studied iron ore, while further detailed automated mineralogical information was required to make sure about the processing units from a practical perspective.

**Keywords:** oolitic iron ore, Gara Djebilet, mineralogical characterization, mineral processing

### 1. Introduction

Iron ore is the main raw material used in iron and steel productions confirmed as a significant resource for both the economy and society (Li et al., 2020). Iron and copper ores make up more than half of all metal ores that are extracted globally (Nakajima et al., 2018). In recent years, the world's large infrastructure has increased the demand for iron ore and steel products (Wu et al., 2016), and there are forecasts that by 2023, steel demand will see a 2.3% rebound to reach 1,822.3 Mt and will grow by 1.7% to 1,854.0 Mt in 2024 (World Steel Association, 2022). Global steel production is expected to increase at

the current pace until reaching 2.065 Mt in 2030. After that, it will slow down and reach a maximum of 2.336 Mt in 2040 (Lopez et al., 2022), which means an increased global demand for iron ore over the coming decades.

With these requirements for iron ore, and as the steel industry develops, the use of iron ore, which is of high quality and easy to handle, gradually declines. That leads to the extraction of iron ore deposits with more complex mineralogies and a higher level of impurities (Silva et al., 2020). Many types of iron ore deposits have historically been significant as iron sources containing hematite, magnetite, titanomagnetite, and pisolitic ironstone (Clout and Manuel, 2015). This last type of ores is widely distributed in South China (Li et al., 2021), Germany, Australia, Canada, Colombia, and the United States (Quast, 2018). Characterization of ores is an integral part of mineral processing because it is the key to choosing the most appropriate route for the recovery of ores. Specifically, this type of ore where its peculiar characteristics complicate processing and resist conventional mineral processing methods (Quast 2018; Gholami et al., 2022). Further detailed information regarding various iron processing routes suitable for several iron ore types is presented elsewhere (Ripke et al., 2019).

Oolitic iron ores are formed from ooids comprised of many concentric layers, with 0.4 to 1.1 wt% phosphorus mostly occurring as apatite. Because of their poor liberation and fine distribution of iron particles, these ores have yet to be economically exploited. (Song et al., 2013). The modern steel industry has limited the concentration of phosphorus in steel to less than 0.04 wt% and this is because of their harmful effects on the mechanical properties of steel (Tang et al., 2013). As a result, phosphorus must typically be removed from phosphorus-rich iron ores before they can be used as feedstock for manufacturing iron. (Li et al., 2015). The acceptable levels of phosphorus in a hot metal range from 0.08 to 0.14; therefore, it is desirable to use iron ores with very low phosphorus contents for steelmaking. Iron ores can be divided into low-phosphorus ore (<0.07% P), medium-phosphorus ore (0.07-0.10% P), and high-phosphorus ore (> 0.10% P) categories depending on the amount of phosphorus they contain (Cheng et al., 1999; Fisher-White et al., 2012). For example, it is well known that for DRI (direct iron reduction) processes the pellets should contain the following chemical properties Fe= minimum 67%,  $\text{SiO}_2 + \text{Al}_2\text{O}_3$ =maximum 3%, S=maximum 0.008%, P=0.03% and  $\text{TiO}_2$ =0.15% (Lu et al., 2015).

Proper knowledge of the chemical and mineralogical characteristics of valuable and gangue minerals is the key to developing the efficient beneficiation of oolitic iron ores. Various analytical techniques can be used to characterize iron ores, among which X-ray Diffraction (XRD), X-ray fluorescence spectrometry (XRF), chemical analyses, and scanning electron microscopy (SEM) are the most common ones. These methods provide critical information on mineralogical distribution, texture, and liberation degree that are key information to elaborate an efficient processing schema (Gholami et al., 2022; Quast, 2018). Clout and Manuel (2015) published a comprehensive review on the mineralogical, chemical, and physical characteristics of different iron ores. They classified mineralogical, petrological, and chemical properties of various iron ores beside some other physico-mechanical characteristics that are necessary for designing a good beneficiation process, including relative hardness, compressive strength, and particle size. Useful research works on the application of XRD characterization of iron ores by de Villiers and Lu (2015), automatic optical image analysis of iron ore by Donskoi et al. (2015), SEM-aided quantitative characterization by Tonzetic (2015), and spectroscopic techniques by Ramanaidou et al. (2015) have been also addressed in the literature. Literature review revealed that most of the research studies on oolitic iron ores deal with particle size and chemical analyses, often accompanied by XRD-based mineralogical studies and there is a big gap in detailed mineralogical information on such iron resources. Sun et al. (2013) and Song et al. (2013) performed simple chemical and XRD analyses to characterize oolitic iron ores from a reservoir in China for the development of a potential processing route. They showed that the contents of  $\text{Al}_2\text{O}_3$  (3-6%) and  $\text{SiO}_2$  (21-22%) respectively in the form of quartz and chamosite, which are detrimental to the efficient recovery of iron, where high phosphorus was the primary harmful element and principally distributed in apatite. Studies on chemical and mineralogical characterization of Australian oolitic iron ores reviewed by Beattie et al. (2017) revealed that there are mild conditions with those ores with relatively high contents of  $\text{Al}_2\text{O}_3$  (1.56%) and  $\text{SiO}_2$  (4.7%) and LOI (Loss on Ignition) value of 9.0%. Novoselov et al. (2018) characterized an oolitic iron ore in Russia using conventional chemical and instrumental methods and showed that the studied ore sample was rich in quartz (32.55%) with relatively high contents of alumina (4.43%) and phosphorous

(0.58%). Recently, Junhui et al. (2020) performed a detailed mineralogical study on a refractory high-phosphorous oolitic iron ore in China. They showed that the main gangue mineral in the ore was quartz (13.41%), with minor amounts of calcite, dolomite, chlorite, hydromica, and collophanite. The contents of alumina and phosphorous were about 6.5% and 1.5%, respectively. Monzavi and Raygan (2020) beneficiated an oolitic-iron ore (containing 45.46wt%  $\text{Fe}_2\text{O}_3$ ) by magnetization roasting (at 625 °C for 25 min) and dry magnetic separation (2500 G).

Currently, the ooidal ironstone deposits are widespread in the south of Algeria and also compose two of the greatest known giant deposits of ooidal ironstones in North Africa i.e., Gara Djebilet and Mechri Abdel Aziz in Tindouf (ANAM et ASGA, 2019). The ore of these deposits often has an oolitic structure, where the intercalation relationship between iron minerals and gangue minerals is complicated and the phosphorus content is high. However, it is necessary to characterize the ore to determine its grade on the iron and other mineral contents, as well as to know about its texture and the nature of gangues associates. Therefore, this research investigation aims to obtain the mineralogical and morphological characterizations of the Gara Djebilet oolitic iron ore. The studies were implemented by X-ray diffraction (XRD), X-ray fluorescence spectrometry (XRF), scanning electron microscopy (SEM), and optical microscopy. Then, potential conceptual scenario was suggested for the recovery of iron from the studied ore based on mineralogical and chemical results.

## 2. Materials and methods

### 2.1. Site description

The oolitic iron ore deposit in the Gara Djebilet area represents the largest and the major iron ore deposit in Algeria and North Africa (Taib, 2009). As seen in Fig. 1, the research area includes the southwest portion of the Tindouf basin, 130 km southeast of the city of Tindouf, and close to the Algerian-Mauritanian border. The East-West area, which spans a distance of around 60 Km, has three significant distinct deposits that have been identified. The 1.7 billion tons of iron-rich, exploitable deposits in Gara Djebilet are spread across two significant lenses: the so-called "west" lens, with 780 million tons, and the so-called "center" lens, with 900 million tons. (Bersi et al., 2016). These three lenses have different sizes (7-90 km<sup>2</sup>), and their thickness is not constant and varies up to about 30 m (Guerrak, 1987). The deposits are still present as mesas of mostly argillaceous and sandy sediments interbedded with flat-lying (1.5-2° north dipping) oolitic iron-stone lenses. Three zones may be distinguished within the main body of iron ore: 1- the lower non-magnetitic ore (3-10 m thick, Fe = 54.6%); 2- the magnetitic ore (6-10 m thick, Fe = 57.8%), which corresponds to the main economic ore; and 3- the upper non-magnetitic ore (4-12 m thick, Fe = 53%) (Guerrak, 1988).

### 2.2. Sampling procedure

the ironstone samples utilized in this study were collected from the Gara Djebilet deposit in the Algerian province of Tindouf, such that to cover as much of the study region as possible while maintaining an acceptable degree of dependability. These lumps were gathered from the old mine and the pits SP2, SP3, SP4, SP5 at the gara west from the magnetitic ore, which corresponds mainly to the workable ore (cutoff grade at 57%), and from gara center with particle size in the range of 0-170 mm. The iron ore lumps were reduced to finer sizes using a sledgehammer. Chosen samples were taken from the received sample for the preparation of polished sections and thin blades. Sub-samples were further crushed to 5 mm using a jaw laboratory crusher (48-D0530/A model of Controls Group), and then mixed and split by quartering technique to obtain a representative sample. After that it was pulverized using a bench-top ring mill (produced by Rocklabs, New Zealand) to obtain fine powder (<74 μm) which was used for chemical and mineralogical analyses.

### 2.3. Characterization methods

The research methods applied in this work were optical microscopy, petrographic microscopy, X-ray fluorescence spectrometry, X-ray diffraction spectrometry, and scanning electron microscopy with energy dispersive X-ray spectrometry (SEM-EDX).

### 2.3.1. Textural and petrographic analysis

For the identification of texture, polished sections were prepared and investigated with a Nikon Eclipse LV150N optical microscope. The petrographic microscope Axiolab 5 was used to visually identify the minerals present in the iron ore samples. Thin blades of the samples were formed and examined under the combination of both plane and cross-polarised light of the microscope. The petrographic investigation was performed at the Laboratory of thin sections in the Geology Department, Badji Mokhtar University, Annaba, Algeria.

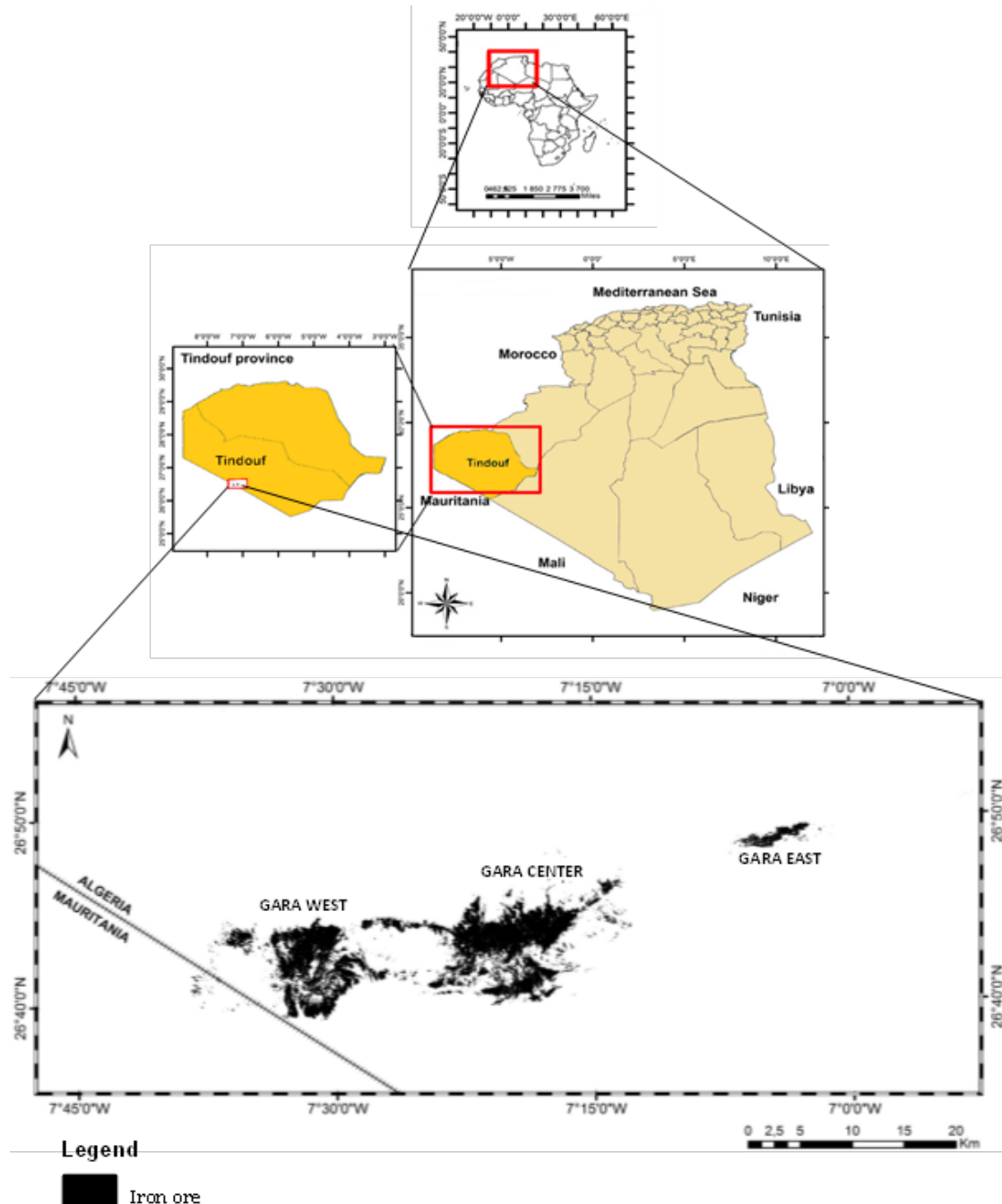


Fig. 1. Location map of study area (modified from Bersi et al., 2016)

### 2.3.2. Chemical analysis

A pressed pellet prepared from a representative sample was analyzed for its major oxides ( $\text{Fe}_2\text{O}_3$ ,  $\text{SiO}_2$ ,  $\text{Al}_2\text{O}_3$ ,  $\text{MnO}$ ,  $\text{MgO}$ ,  $\text{CaO}$ ,  $\text{K}_2\text{O}$ ,  $\text{Na}_2\text{O}$ ,  $\text{TiO}_2$ , and  $\text{P}_2\text{O}_5$ ) by the XRF technique using a Bruker-Axs: S8 TIGER X-ray spectrometer. Loss on ignition (L.O.I.) was obtained by heating the sample powder to 1000

°C for 2 h (Fozooni et al., 2017). The micro-morphology and the dispersion state of the minerals in the iron ore were observed using a scanning electron microscope (SEM, Quanta 250 model) combined with EDS, and with the advantages of high magnification, clear image, and simple operation.

### 2.3.3. Mineralogical analysis

X-ray diffractometer (XRD), Bruker D8 ADVANCE model, equipped with Copper Anticathode in configuration Bragg-Brentano optics with fixed slits, Ni filter, and ultrafast linear detector was used for mineralogical analysis. The radiation employed was a Cu K- $\alpha$  with a wavelength of 1.540598 Å within the values of  $2\theta$  from 0 – 80° Bragg's angle (Khoshdast and Shojaei, 2012). The XRD was used to identify the mineral phases present in the ore. The mass of sample was required to be about 3 g with a particle size of <74  $\mu\text{m}$ . The sample was pressed to obtain a flat and uniform surface and after that it was put into the XRD equipment to start detection (Hasanizadeh et al., 2023). The XRF and XRD investigations were performed at the Technological platform "Development of Materials and Manufacturing", National Polytechnic School, Constantine, Algeria.

## 3. Results and discussions

### 3.1. X-ray fluorescence spectroscopy

The results of chemical analysis by the X-ray fluorescence (Table 1) indicate that the Gara Djebilet iron ore contains 56.58 wt% of iron.  $\text{Fe}_2\text{O}_3$ ,  $\text{SiO}_2$ , and  $\text{Al}_2\text{O}_3$  are the most abundant oxides, making up more than 90% of the oxides and indicating the presence of quartz and hematite in the ore. However, associate elements such as phosphorus are considered to be deleterious since it is higher than the recommended benchmarks. The phosphorus content of Gara Djebilet iron ore is 0.921 wt%, which makes it a high-phosphorous iron ore (>0.1% P) and presents a challenge that requires better beneficiation techniques for its reduction. Additionally, as seen in Table 1, this iron ore has a significant concentration of impurities including  $\text{TiO}_2$ ,  $\text{MnO}$ , and  $\text{MgO}$  whereas other oxides are present at negligible levels. Because of the iron ore's high gangue content and lack of commercially graded blast furnace ore quality, its exploration can only be helpful for the manufacture of direct reduction iron; 4%  $\text{Al}_2\text{O}_3$ , and 6%  $\text{SiO}_2$  (Joan et al., 2015).

Table 1. Chemical composition of Gara Djebilet iron ore sample by the XRF method

Element	TFe	$\text{Fe}_2\text{O}_3$	$\text{SiO}_2$	$\text{Al}_2\text{O}_3$	CaO	$\text{P}_2\text{O}_5$	MnO	MgO	$\text{TiO}_2$	$\text{Na}_2\text{O}$	$\text{K}_2\text{O}$	$\text{As}_2\text{O}_3$	*LOI
Content (wt %)	56.58	80.9	7.98	7.09	1.03	0.921	0.6	0.517	0.225	0.0826	0.0529	0.0471	4.9

\* LOI is the percentage of mass lost on ignition at 1000 °C

### 3.2. Optical and petrographic microscopy

Fig. 3 depicts the findings from optical microscope observations of polished cross sections of the ore, which reveal the ore's oolitic structure, which is made up of lighter spherical grains arranged in concentric layers contained in a darker matrix. The ore's appearance is consistent with its oolitic ore structure. The oval-shaped ooids that make up the oolitic texture range in size from 150  $\mu\text{m}$  to 800  $\mu\text{m}$ . Those ooids are containing hematite, goethite, and magnetite along with impurity elements such as silicon and phosphorus.

Gara Djebilet iron ore is brownish red of oolitic texture and semi-hard. The petrographical and mineralogical studies of rocks are shown in Figs. 4 and 5. The photomicrographs of thin sections (Fig. 4) show that the ironstone is dominated by the mineralogic magnetite-rich association, and two iron ore facies types: facies with scattered ooids in a quartz-poor groundmass (non-detrital facies: FOND) as shown in (Fig. 4a), and facies with cemented jointed ooids and pore-filling structures (cemented facies: FOC) as shown in (Fig. 4b). The predominant cement component in the FOC facies type is oxidized (goethite with a brownish-yellow tint). The iron ore minerals can appear in a variety of ways, including as the small automorphic crystals (5–20  $\mu\text{m}$ ) known as magnetite that are found within ooids underlining the oolitic structure (Fig. 5a) and as larger automorphic crystals (50–100  $\mu\text{m}$ ) in the

groundmass that are opaque and has no cleavage under the microscope as shown in (Fig. 4a). Within the shallower parts of the magnetitic ore, maghemite is commonly found. It grows at its cost and occurs inside magnetite. (Fig. 4a).

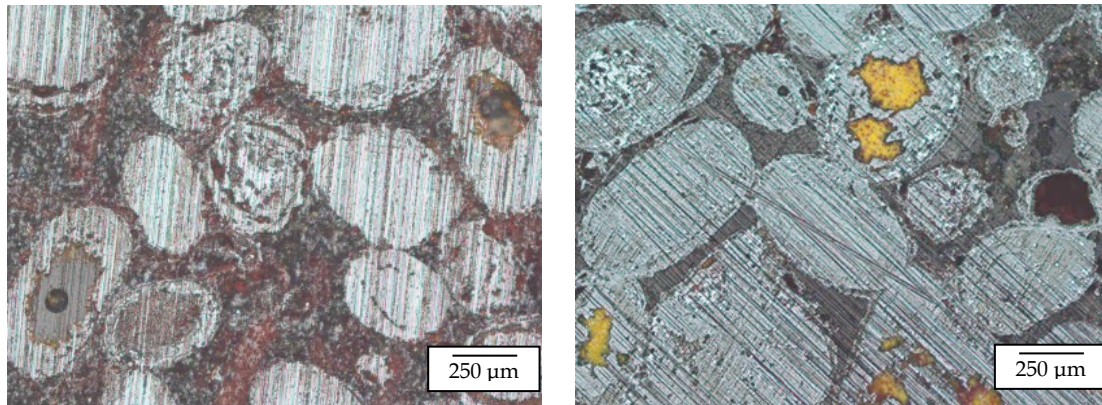


Fig. 3. Photomicrographs of bulks of Gara Djebilet iron ore sample mounted on epoxy and polished. The largest (ooid) grain measures 800 µm in diameter

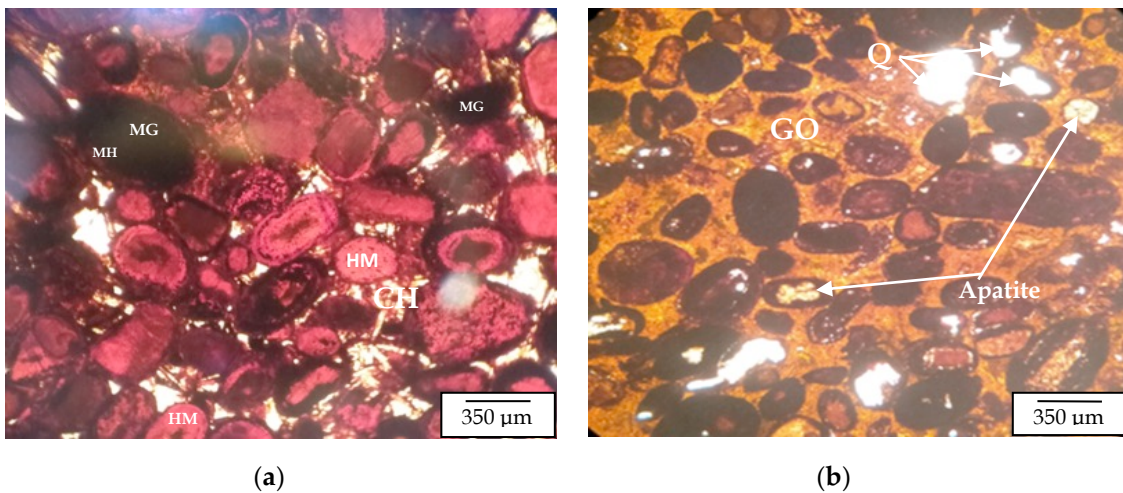


Fig. 4. Photomicrographs of thin sections of Gara Djebilet iron ore X10 PL. HM–Hematite, MG–Magnetite, MH–Maghemite, GO–Goethite, CH–Chamosite, Q–Quartz

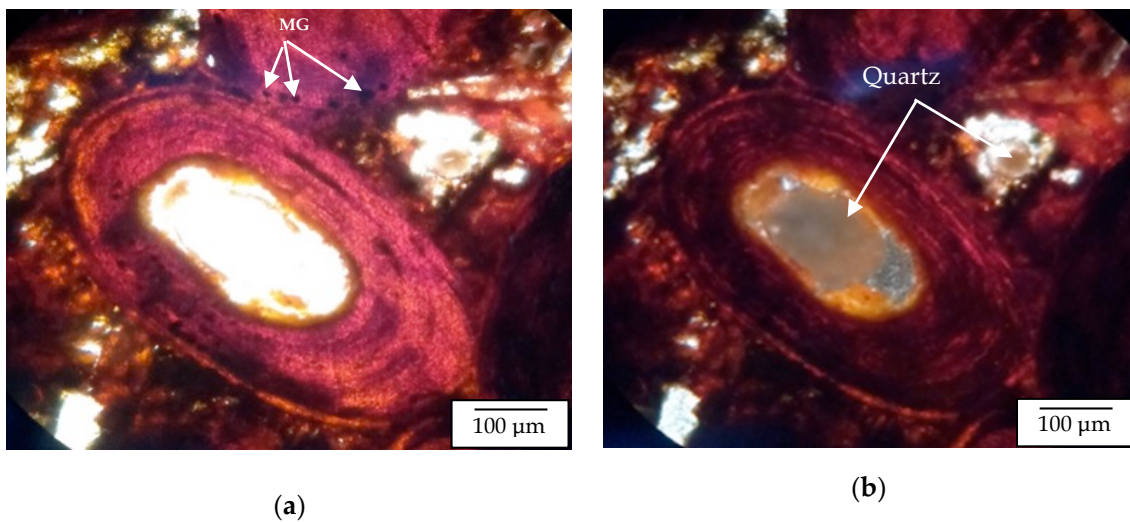


Fig. 5. Photomicrograph of a thin section of Gara Djebilet iron ore shows Oolite with quartz nuclei ((a) X50 PL, (b) X50 PAL)

Chamosite is found in ooids and groundmass in various ways; in Fig. 4a, it is visible as fibrous minerals in the groundmass. All types of iron ore contain hematite, which is tightly connected to chamosite or alternates throughout the layers of ooids. It reflects as a vivid red color, as seen in Fig. 4a (hematitic ooids). Non-ferruginous minerals. Apatite is quite scarce that frequently appears as prismatic crystals in both ooids and groundmass. It is bright-yellow emission (Fig. 4b). Quartz as nuclei or detrital grains has weak birefringence (Fig. 5b).

The observation of the photomicrographs and the granulochemical analyses (Table 2) allows the determination of the liberation size of iron and gangue minerals, particularly that of phosphorus containing oolitic particles. The phosphorus mineral in the ore mainly exists in the form of collophane, a variety of apatite, which can be divided into three types. The first type, known as block collophane, occurs in debris and cement and has a particle size of 20  $\mu\text{m}$  to 200  $\mu\text{m}$ , making it easy to remove. The second type, called band collophane, is more difficult to liberate as it is distributed within the banded oolitic structure. The third type of phosphorus mineral is dispersed within hematite crystals (Figure 4b, 8b) (Chen et al., 2023). Thus, the liberation size of phosphorus mineral is very fine and ranging from 0,1  $\mu\text{m}$  and 10  $\mu\text{m}$ . With hematite crystals size of less than 0.05 mm.

Table 2 shows a decrease in the content of total iron and  $\text{Fe}_2\text{O}_3$  in the fine size classes [-0.25 mm, +0.125 mm], [-0.125 mm, +0.063 mm], and [-0.063 mm] and, in return, an increase in the contents of gangue minerals  $\text{Si}_2\text{O}$ ,  $\text{Al}_2\text{O}_3$  and  $\text{P}_2\text{O}_5$ . This means that the liberation size of gangue minerals and chamosite starts from -125  $\mu\text{m}$  (Table 2, Fig. 6). The liberation rate of iron and gangue minerals is 100% at the size less than 10  $\mu\text{m}$ .

The results of the sieve analysis (Table 2) show that the mass is distributed between the larger fractions [+2, +1, +0.5 and +0.25 mm], and the finer fractions [+0.125, +0.063 and -0.063 mm], which confirms that the iron ore of Gara Djebilet is semi-hard.

Table 2. Granulochemical analysis of Gara Djebilet iron ore sample by particle size analysis and XRF method

Designation	>2mm	-2mm+1mm	-1mm+0.5mm	-0.5 mm+0.25mm	-0.25mm +0.125mm	-0.125 mm+0.063	<0.063mm
Weight (g)	204,58	71,57	48,27	42,52	46,76	56,17	30,13
Total 500							
TFe	57.91	57.28	57.49	57.21	53.7	53.9	54.55
$\text{Fe}_2\text{O}_3$	82.8	81.9	82.2	81.8	76.8	77.1	78.0
$\text{SiO}_2$	7.22	7.59	7.4	7.61	9.69	9.51	9.15
$\text{Al}_2\text{O}_3$	6.32	6.69	6.6	6.72	8.74	8.54	8.07
CaO	0.731	0.823	0.836	0.913	1.37	1.59	1.48
$\text{P}_2\text{O}_5$	0.882	0.901	0.88	0.863	1.02	1.06	1.05
MgO	0.461	0.467	0.446	0.458	0.576	0.569	0.522
$\text{TiO}_2$	0.229	0.233	0.227	0.241	0.235	0.234	0.215
$\text{Na}_2\text{O}$	0.069	0.087	0.084	0.083	0.104	0.09	0.224

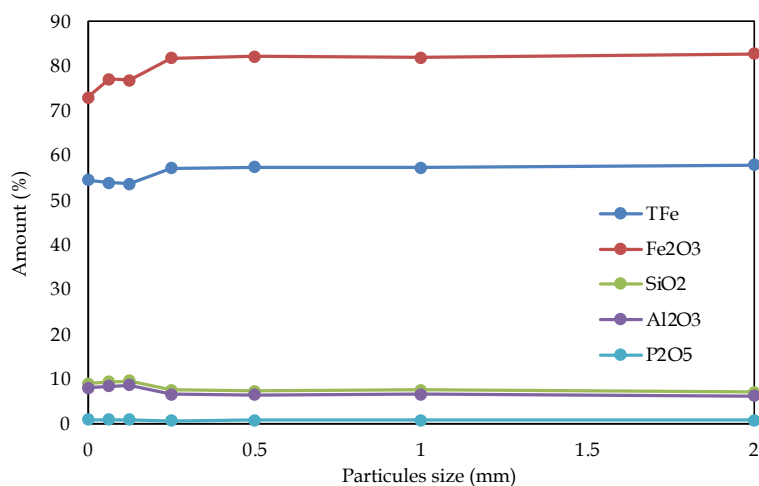


Fig. 6. Graphical representation of granulochemical analysis results

### 3.3. Powder X-ray diffraction results

To find out the types of minerals in the raw material, the mineral phase of the iron ore sample was qualitatively analyzed using an X-ray diffractometer. As shown in Fig. 7, the XRD analysis confirmed the presence of iron oxide (hematite  $\text{Fe}_2\text{O}_3$ ) as the major phase along with magnetite ( $\text{Fe}_3\text{O}_4$ ), goethite ( $\text{FeO}(\text{OH})$ ), chlorite in the form of chamosite ( $(\text{Mg,Fe,Al})_6(\text{Si,Al})_4\text{O}_{10}(\text{OH})_8$ ), siderite ( $\text{FeCO}_3$ ) and quartz ( $\text{SiO}_2$ ). Due to the low content of other minerals as apatite, they could not be displayed in the XRD spectrum. The semi-quantitative results of XRD show that the mass fractions of hematite, magnetite, goethite and siderite making above of 80%, which hematite is the dominant phase.

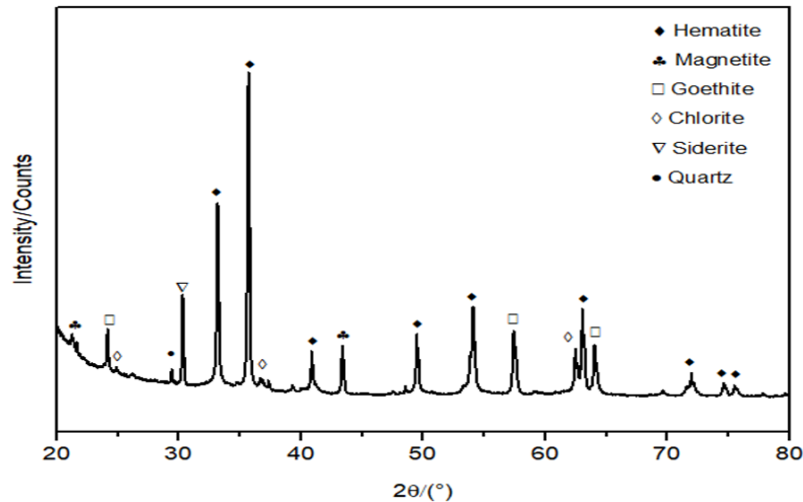


Fig. 7. XRD pattern of Gara Djebilet oolitic iron ore

### 3.4. Scanning electron microscope with energy dispersive X-ray spectrometry

To confirm the results obtained previously of raw material samples and the thin sections, some SEM images were taken. The results are illustrated in Fig. 8. Fig. 8a confirms that its unique concentric oolitic structure, in which iron and gangue minerals are embedded. There are three phases observed and represented by grey, dark grey and black, where hematite, goethite and magnetite (grey colour), fluorapatite (dark grey colour), chlorite (chamosite) (black colour). These results are in good agreement with XRD and petrographic results. The Fig. 8b and 8c exhibits that phosphorous is distributed in both the ooids and the groundmass. Fig. 8d shows that iron ore contains phosphorus and Fig. 8e shows that Al, Mg and Si distribute in chlorite (chamosite).

### 3.5. Proposed scenarios for processing of Gara Djebilet iron ore

The results proved that the beneficiation of the Gara Djebilet iron ore is potentially expected to be extremely difficult. This is mainly related to the distribution of phosphorus throughout the sample and the dissemination of iron minerals as well as their presence in finer fraction sizes. So far, there have been several studies in the field of processing oolitic iron ores, which were briefly reviewed by Quast (2018). According to the reported processing methods as well as the mineralogical and petrological results presented, a conceptual approach can be suggested for the processing of Gara Djebilet iron ore: fine comminution-reduction roasting-low intensity magnetic separation-fatty acid reverse flotation. The first point is the need to pay attention to the complexity of the mineralogical texture and the necessity to increase the degree of liberation in fine particle size. Therefore, fine comminution and efficient classification will be integral parts of any proposed processing process (Jarkani et al., 2014). The necessity of fine grinding has also been emphasized by other researchers (Hanna and Anazia, 1990).

Considering that the dominant iron mineral is hematite, it is necessary to transform it with the other iron minerals to magnetite. One of the efficient methods to convert hematite to magnetite is to use reduction roasting. This method may be used in single or in combination with hydrometallurgical

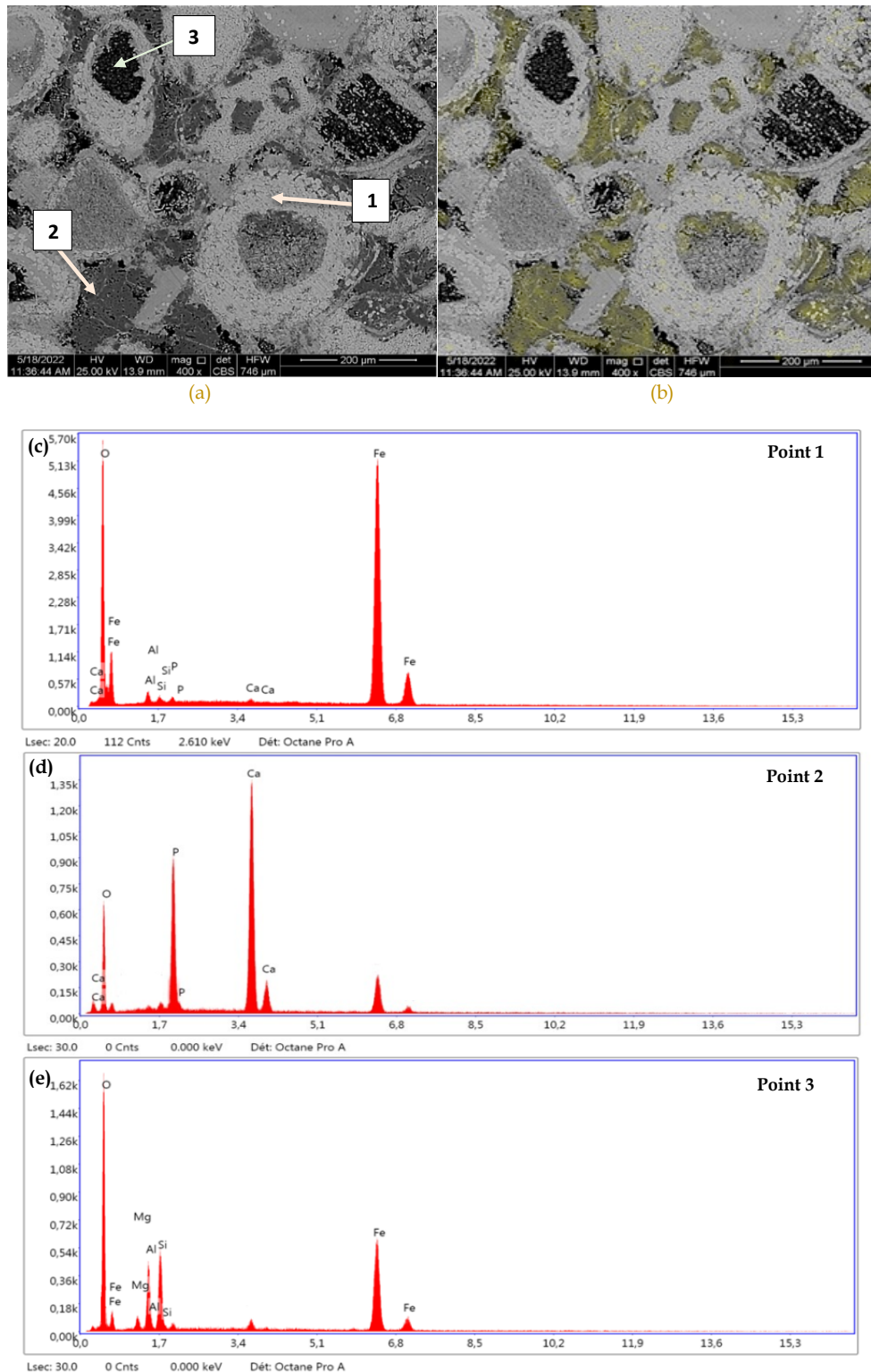


Fig. 8. Micrographs of Gara Djebilet oolitic iron ore: (a) SEM image, (b) distribution of phosphorus, (c) iron minerals, (d) fluorapatite, and (e) chlorite

methods (Guo et al., 2015; Dey et al., 2017; Pan et al., 2022). A great amount of phosphorus can be also removed in the roasting stage by mixing the finely ground ore with a roasting additive like  $\text{Na}_2\text{CO}_3$  or  $\text{Na}_2\text{SO}_4$  (Li et al., 2013; Yu et al., 2014). Although the development of high-gradient magnetic separation technology has significantly reduced the need for relatively expensive thermal roasting, improving ore magnetic properties can still be of great interest to processing engineers. For this reason, it is possible to convert hematite into magnetite with a roasting pretreatment step and then concentrate the ore by using

low-intensity magnetic separation (LIMS). At this stage, it is expected that a large proportion of the gangue minerals, the majority of which is quartz, and amount of phosphorus will be removed. Then, if needed, the silica and phosphorus content of the concentrate can be reduced with a reverse flotation step (Rao et al., 2013; Quast, 2017), because apatite has a relatively hydrophobic nature that helps improve flotation efficiency. For this, conventionally used mechanical and column flotation cells combined with a cavitation tube or even intensified flotation equipment which are more effective for finely disseminated particles can be applied (Hassanzadeh, 2023).

It should be noted that the above processing method is proposed based on the characteristics of the investigated iron ore and the available technologies in Algeria. There is no room for doubt that to evaluate their efficiency, laboratory studies and large-scale validations are needed.

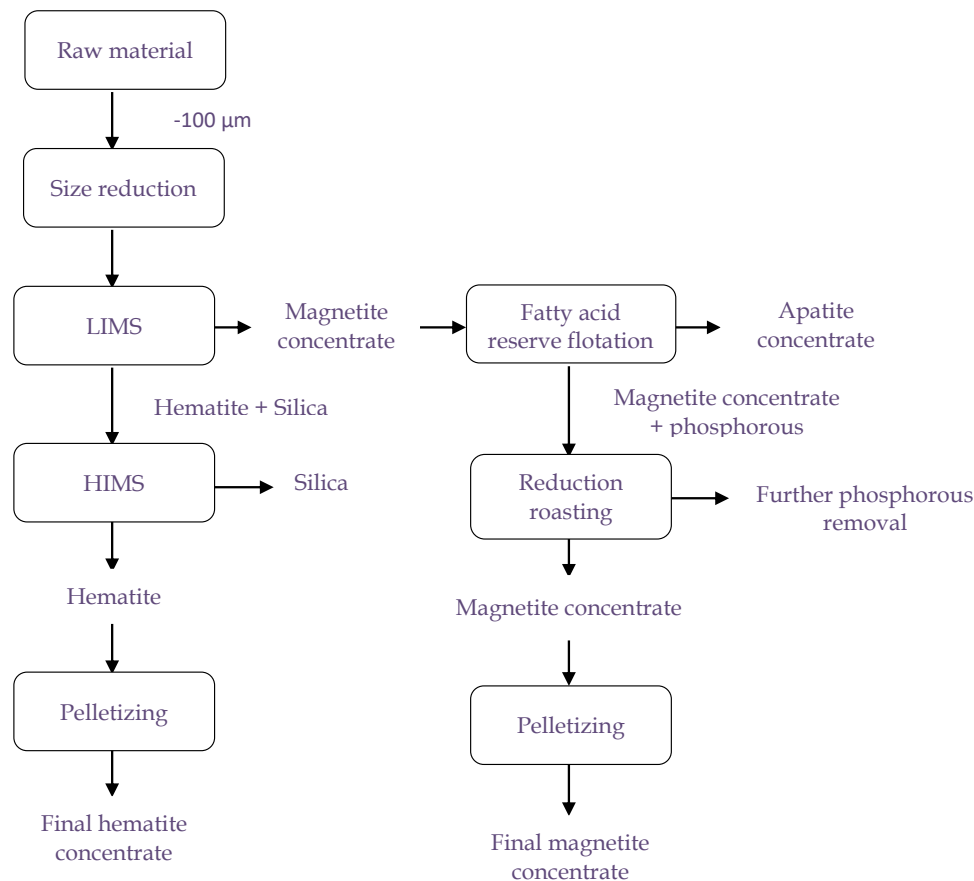


Fig. 9. Proposed method for processing of Gara Djebilet iron ore

#### 4. Conclusions

Gara Djebilet iron ore, a high-phosphorus iron ore, has been characterized using a variety of analytical techniques (XRF, XRD, SEM-EDX and optical, petrographical microscopies) in an attempt to unravel the presentation and distribution of the iron and gangue minerals in the ore. The existence of phosphorus was confirmed by the findings of these investigations, its concentration in the sample studied was determined to be 0.921 wt%. It occurred in higher concentration compared to the limit of phosphorus in the steel. Its spatial distribution in the ore was demonstrated to be in both the ooids and the groundmass. Total iron (TFe) existed in the form of hematite, magnetite, goethite, and siderite. Al, Mg, Si were distributed in chamosite, while SiO<sub>2</sub> was present as quartz. It was found based on the mineralogical and petrological results that the phosphorus can be removed from iron ore by very different routes of treatment, however with variable dephosphoration rates. According to the mineralogy of the Gara Djebilet iron ore, thermal or mixed processes were closer to reality technical solutions and can remove phosphorus from the ore to meet market specifications of 0.08 wt% P, because the thermal processing disrupts the structure of goethite FeO(OH) is effective in releasing phosphorus associated with this mineral and becoming available to be extracted by a leaching solution. We believe

that these data will be extremely helpful in developing successful beneficiation and phosphorus removal strategies. Finally, a conceptual flowsheet was proposed for the recovery of iron from the studied ore based on characterization results. However, further experimental investigations including mineralogical analyses using automated mineralogy as well as systematic ore dressing processes are necessary to confirm the effectiveness of the suggested beneficiation process.

### Acknowledgments

The authors express their gratitude to the Laboratory of thin sections in the Geology Department, Badji Mokhtar University, as well as to the Mining, Metallurgy and Materials Laboratory L3M, National Higher School of Technology and Engineering, Annaba, Algeria, for their support to realize this research study.

### References

- ANAM, ASGA, 2019. *Inventaire des substances minérales métalliques ferreuses et non ferreuses de l'Algérie*, réalisé par la ministère de l'énergie et des mines en collaboration avec l'agence du service géologique de l'Algérie 2019. pp. 75–120.
- BEATTIE, E., PLAZEK, C., BLAKE, K., 2017. *Dirty goethite- a geochemical characterization of some western Robe River channel iron deposits*. In: Proceedings, Iron Ore 2017. Australasian Institute of Mining and Metallurgy, pp. 489–502.
- BERSI, M., SAIBI, H., CHABOU, M.C., 2016. *Aerogravity and remote sensing observations of an iron deposit in Gara Djebilet, southwestern Algeria*. Journal of African Earth Sciences. 116, 134–150.
- CHEN, C., ZHANG, Y., ZOU, K., ZHANG, F., 2023. *Flotation Dephosphorization of High-Phosphorus Oolitic Ore*. Minerals. 13, 1485.
- CHENG, C.T., MISRA, V.N., CLOUGH, J., MUNI, R., 1999. *Dephosphorisation of Western Australian iron ore by hydrometallurgical process*. Minerals Engineering. 12, 1083–1092.
- CLOUT, J.M.F., MANUEL, J.R., 2015. *Mineralogical, chemical and physical characteristics of iron ore*. In : Lu, Liming (Ed.), Iron Ore : Mineralogy, Processing and Environmental Sustainability. Elsevier, pp. 45–84.
- DE VILLIERS, J.P.R., LU, L., 2015. *XRD analysis and evaluation of iron ores and sinters*. In: Lu, Liming (Ed.), Iron Ore: Mineralogy, Processing and Environmental Sustainability. Elsevier, pp. 85–100 (Chapter 3).
- DEY, S., MOHANTA, M.K., SINGH, R., 2017. *Mineralogy and textural impact on beneficiation of goethitic ore*. International Journal of Mining Science and Technology. 27, 445–450.
- DONSKOI, E., POLIAKOV, A., MANUEL, J.R., 2015. *Automated optical image analysis of natural and sintered iron ore*. In: Lu, Liming (Ed.), Iron Ore: Mineralogy, Processing and Environmental Sustainability. Elsevier, pp. 101–160 (Chapter 4).
- FISHER-WHITE, M.J., LOVEL, R.R., SPARROW, G.J., 2012. *Phosphorus removal from goethitic iron ore with a low-temperature heat treatment and a caustic leach*. ISIJ Int. 52, 797– 803.
- FOZOONI, S., KHOSHDAST, H., HASSANI, H., HAMIDIAN, H., 2017. *Synthesis of oxazolone and imidazolone derivatives in presence of H<sub>2</sub>O<sub>2</sub> promoted fly ash as a novel and efficient catalyst*. Journal of Sciences. 28(3), 221–230.
- GHOLAMI, A.R., ASGARI, K., KHOSHDAST, H., HASSANZADEH, A., 2022. *A hybrid geometallurgical study using coupled Historical Data (HD) and Deep Learning (DL) techniques on a copper ore mine*. Physicochemical Problems of Mineral Processing. 58(3), 147841.
- GUERRAK, S., 1987. *Paleozoic oolitic ironstones of the Algerian Sahara: a review*. Journal of African Earth Sciences. 6 (1) 1–8.
- GUERRAK, S., 1988. *Geology of the early Devonian oolitic iron ore of the Gara Djebilet field, Saharan Platform, Algeria*. Ore Geol. Rev. 3 (4), 333–358.
- GUO, L., GAO, J., ZHONG, Y., GAO, H., GUO, Z., 2015. *Phosphorus removal from high phosphorus oolitic iron ore with acid leaching fluidized-reduction and melt-separation process*. ISIJ International. 55(9), 1806–1815.
- HANNA, J., ANAZIA, I.J., 1990. *Processing of hematitic iron ores*. In: Hanna, J., Attia, Y.A. (Eds.), Advances in Fine Particles Processing. Elsevier, New York, pp. 413–425.
- HASANIZADEH, I., KHOSHDAST, H., ASGARI, K., HUANG, Q., RAHMANIAN, A., 2023. *Studying the influence of cationized pyrolysis oil on the flotation of a bituminous coal using historical data design*. International Journal of Coal Preparation and Utilization. DOI: <https://doi.org/10.1080/19392699.2023.2254708>

- HASSANZADEH, A., 2023. A short pragmatic overview on the development of flotation machines from historical, mechanical, and metallurgical perspectives, Proceedings of 9<sup>th</sup> International Congress of Mining, Machinery and Technologies, September 13-15, Izmir, Türkiye, 10-15.
- JARKANI, S.A., KHOSHDAST, H., SHARIAT, E., SAM, A., 2014. *Modeling the effects of mechanical parameters on the hydrodynamic behavior of vertical current classifiers*. International Journal of Mining Science and Technology. 24(1), 123-127.
- JOAN, J.K., ALEX, M.M., AUGUSTINE, B.M., STEPHEN, K.K., 2015. *Characterization of selected mineral ores in the Eastern Zone of Kenya: Case study of Mwingi North Constituency in Kitui County*. Int. J. Mining Eng. Mineral Proc. 4 (1) 8-17.
- JUNHUI, X., KAI, Z., ZHEN, W., 2020. *Studying on mineralogical characteristics of a refractory high-phosphorous oolitic iron ore*. SN Applied Sciences. 2, 1051.
- KHOSHDAST, H., 2019. *Practical problems in froth flotation*. Hormozgan University Press, Tehran, Iran.
- KHOSHDAST, H., SAM, A., 2012. *An efficiency evaluation of iron concentrates flotation using rhamnolipid biosurfactant as a frothing reagent*. Environmental Engineering Research. 17(1), 9-15.
- KHOSHDAST, H., SHOJAEI, V., 2012. *Ash removal from a sample coal by flotation using rhamnolipid biosurfactants*. Journal of Mining World Express. 1(2), 39-45.
- LI, D., MOGHADDAM, MR., MONJEZI, M., DANIAL J. A., AMIRHOSSEIN M. 2020. *Development of a Group Method of Data Handling Technique to Forecast Iron Ore Price*. Applied Sciences. 10 (7) 23-64. MDPI.
- LI, G., RAO, M., OUYANG, C., ZHANG, S., PENG, Z., TAO., 2015. *Distribution characteristics of phosphorus in the Metallic Iron during Solid-State Reductive Roasting of Oolitic Hematite Ore*. ISIJ International. 55 (11), 2304-2309.
- LI, F., ZHANG, P., MA, X., YUAN, G., 2021. *The iron oolitic deposits of the lower Devonian Yangmaba formation in the Longmenshan area, Sichuan Basin*. Marine and Petroleum Geology. 130, 105-137.
- LI, G., ZHANG, S., RAO, M., ZHANG, Y., JIANG, T., 2013. *Effects of sodium salts on reduction roasting and Fe-P separation of high-phosphorus oolitic hematite ore*. International Journal of Mineral Processing. 124, 26-34.
- LOPEZ, G., FARFAN, J., BREYER, C., 2022. *Trends in the global steel industry: Evolutionary projections and defossilisation pathways through power-to-steel*. Journal of Cleaner Production. 375, 134-182.
- LU, L., PAN, J., ZHU, D., 2015. *Quality requirements of iron ore for iron production*, Iron Ore. 475-504.
- MONZAVI, M., and RAYGAN, Sh., 2020, *Beneficiation of an Oolitic-iron ore by magnetization roasting and magnetic separation*, Iranian Journal of Materials Science & Engineering, 17(3), 17-29.
- NAKAJIMA, K., DAIGO, I., NANSAI, K., MATSUBAE, K., TAKAYANAGI, W., TOMITA, M., MATSUNO, Y., 2018. *Global distribution of material consumption: Nickel, copper, and iron*. Resour. Conserv. Recycl. 133, 369-374.
- NOVOSELOV, K.A., BELOGUB, E.V., KOTLYAROV, V.A., FILIPPOVA, K.A., SADYKOV, S.A., 2018. *Mineralogical and Geochemical Features of Oolitic Ironstones from the Sinara-Techa Deposit, Kurgan District, Russia*. Geology of Ore Deposits. 60(3), 265-276.
- PAN, J., LU, S., LI, S., ZHU, D., GUO, Z., SHI, Y., DONG, T., 2022. *A new route to upgrading the high-phosphorus oolitic hematite ore by sodium magnetization roasting-magnetic separation-acid and alkaline leaching process*. Minerals. 12(5), 568.
- QUAST, K., 2017. *An investigation of the flotation minimum in the oleate flotation of hematite under alkaline conditions*. Minerals Engineering. 113, 71-82.
- QUAST, K., 2018. *A review on the characterization and processing of oolitic iron ores*. Minerals Engineering. 126, 89-100.
- RAMANAIDOU, E., WELLS, M., LAU, I., LAUKAMP, C., 2015. *Characterization of iron ore by visible and infrared reflectance and, Raman spectroscopies*. In: Liming, Lu (Ed.), Chapter 6 in, Iron Ore: Mineralogy, Processing and Environmental Sustainability. Elsevier, pp. 191-228.
- RAO, Z.Q., ZHANG, Y.S., JIBN, Y.C., 2013. *Improved flotation of oolitic hematite ore based on a novel cationic collector*. Advanced Materials Research. 303-306, 2713-2716.
- RIPKE, S. Jayson, POVEROMO, J., BATTLE, T.P., WALQUI, H., HASELHUHN, H., and LARSON, M., Iron Ore Beneficiation, 2019. Chapter 12.16. SME Mineral Processing and Extractive Metallurgy Handbook, 1755-1779.
- SILVA, L.M., NASCIMENTO, M., OLIVEIRAC, E.M., QUEIROZ, A.V., FERNANDES, M.T., CASTRO, J.A., 2020. *Evaluation of the Influence of Particle Size in the Acid Baking Process for the Reduction of Phosphorus Content in Iron Ore*. Materials Research. 23(6).
- SONG, S., CAMPOS-TORO, E.F., LÓPEZ-VALDIVIESO, A., 2013. *Formation of micro-fractures on an oolitic iron ore under microwave treatment and its effect on selective fragmentation*. Powder Technol. 243, 155-160.

- SUN, Y.S., HAN, Y.X., GAO, P., WANG, Z.H., REN, D.Z., 2013. *Recovery of iron from high phosphorus oolitic iron ore using coal-based reduction followed by magnetic separation*. International Journal of Minerals, Metallurgy and Materials. 20(5), 411.
- TAIB, M., 2009. *The Mineral Industry of Algeria*. U.S. Geological Survey. Minerals Yearbook Algeria. p.13.
- TANG, H., WANG, J., GUO, Z., OU, T., 2013. *Intensifying gaseous reduction of high phosphorus iron ore fines by microwave pretreatment*. Journal of Iron and Steel Research International. 20 (5), 17-23.
- TONZETIC, I.Z., 2015. *Quantitative analysis of iron ore using SEM-based technologies*. In: Lu, Liming (Ed.), *Iron Ore: Mineralogy, Processing and Environmental Sustainability*. Elsevier, pp. 161-190 (Chapter 5).
- WORLD STEEL ASSOCIATION., 2022. *Total production of crude steel*. ([https://worldsteel.org/steel-by-topic/statistics/annual-production-steel-data/P1\\_crude\\_steel\\_total\\_pub/WORLD\\_ALL](https://worldsteel.org/steel-by-topic/statistics/annual-production-steel-data/P1_crude_steel_total_pub/WORLD_ALL))
- WU, J., YANG, J., MA, L., LI, Z., SHEN, X., 2016. *A system analysis of the development strategy of iron ore in China*. Resour. Policy. 48, 32-40.
- YU, W., SUN, T., CUI, Q., 2014. *Can sodium sulfate be used as an additive for the reduction roasting of high-phosphorus oolitic hematite ore?* International Journal of Mineral Processing. 133, 119-122.